2011 IEEE/RSJ International Conference on
Intelligent Robots and Systems
September 25-30, 2011. San Francisco, CA, USA

State Estimation for Snake Robots

David Rollinson, Austin Buchan, and Howie Choset

Abstract— **We present a comparison of methods to estimate the shape and orientation of a locomoting snake robot by fusing the robot's redundant internal proprioceptive sensors using an Extended Kalman Filter (EKF). All of the estimators used in this work represent the shape of the snake with *gait* parameters to reduce the complexity of the robot configuration space. The compared approaches for representing shape and pose of the snake robot differ primarily in the use of a body frame fixed to the pose of a single module versus one that is aligned with the *virtual chassis*. Additionally, we evaluate a state representation that explicitly tracks joint angles for improved estimates. For one particular gait, rolling, we present experimental data where motion capture data of the snake robot is used as ground truth to compare the accuracy of the state estimates from these techniques. We show that using the virtual chassis body frame, rather than a fixed body frame, results in improved accuracy of the snake robot's estimated pitch and roll. We also show that, in general, representing the robot's shape with gait parameters is sufficient to accurately estimate shape and pose, though it can be improved upon in specific cases by explicitly modeling joint angles.**

I. Introduction

Snake robots are a class of hyper-redundant mechanisms [1] consisting of kinematically constrained links chained together in series. Their many degrees of freedom allow them to navigate a wide range of environments. Our group has developed modular snake robots that rely solely on their internal shape changes to locomote through their environment [2]. To simplify control of the snake's many degrees of freedom, cyclic motions (gaits) have been developed that undulate the snake's joints according to parameterized sine waves [3]. Gaits enable an intuitive mapping between change in a single parameter (gait phase) and motion of the snake through the environment. One such gait that is particularly useful for locomoting on flat surfaces is rolling, where progression through the gait results in translation perpendicular to the robot's long axis.

Currently, human operation of the snake robot consists of specifying gait parameters and phase speed to move in a desired direction. However, remotely operating the snake robot using only the head module video and joint encoders has proven to be difficult. As the snake progresses through the gait cycle, interaction with the ground and position controller lag cause the snake's shape to deviate from the commanded shape. Even with perfect control, the rolling motion causes the operator's camera perspective to tumble rapidly. To address these problems we would like to use on-board position and inertial sensors to estimate two basic aspects of the system: the snake robot's shape and the orientation of that shape with respect to the world.

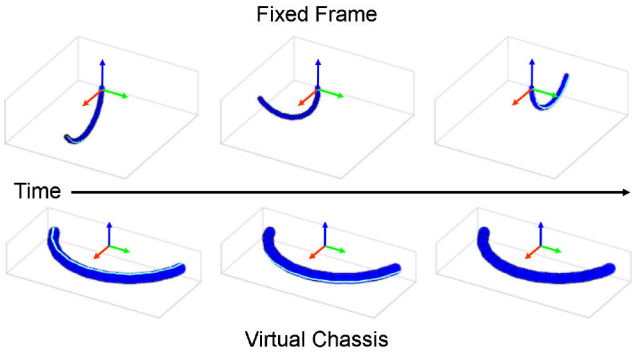

Fig. 1: The two body frames used in state estimation. The upper diagram shows the coordinate frame aligned with the head module of the snake robot. The lower diagram shows the coordinate frame aligned the virtual chassis.

Looking forward to improved human and autonomous operation, we want this pose information to be intuitively related to the motion of the robot as a whole. While joint angles between each link fully describe the shape of the snake, the user's intuition (and indeed the controls of the system) are based in the lower dimensional space of gait parameters. This work uses the same simplifications that gaits allow for control to reduce the state representation of the snake's shape from 16 parameters (one for each joint angle) to 4 (gait parameters and their first derivatives).

Estimating orientation while locomoting is a challenge with snake robots. Part of the complexity lies in the choice of body frame in which to describe the snake robot's motion. Fixing a body frame to a single module means that the internal shape changes vary dramatically within the body frame. Furthermore, an accurate state estimator for the pose of the robot would need the environmental interactions that the robot uses to locomote to be built into the process model.

In order to mitigate the effect of these motions, we define a body frame that is located at the center of mass and aligned with the principal moments of inertia of the shape of the snake [4]. The center of mass can be calculated by averaging the x, y and z positions of the modules in an arbitrary frame, and the principal moments of inertia of the snake can be determined by taking the singular value decomposition (SVD) of the positions of all of the snakes modules. Performing these calculations for a given

David Rollinson is a graduate student in the Robotics Institute, Carnegie Mellon University, Pittsburgh, PA, 15213 drollins@cs.cmu.edu
Austin Buchan is a lab assistant in the Robotics Institute, Carnegie Mellon University, Pittsburgh, PA, 15213 abuchan@cmu.edu
Howie Choset is an associate professor in the Robotics Institute, Carnegie Mellon University, Pittsburgh, PA, 15213 choset@cs.cmu.edu

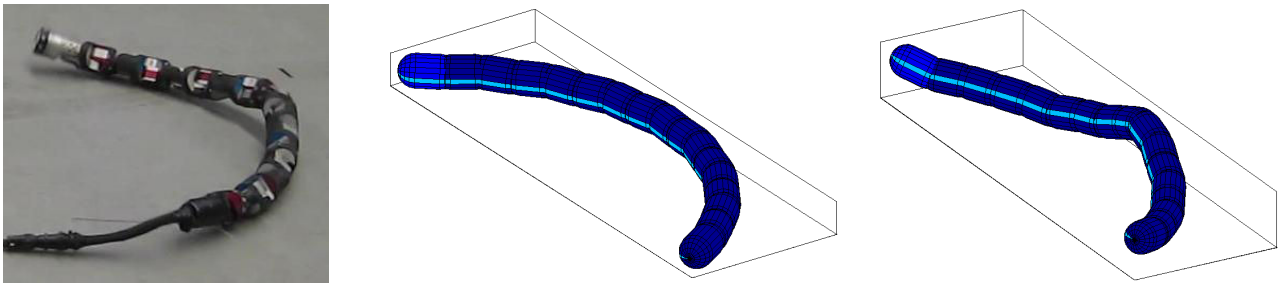

(a) Actual snake shape and pose

(b) Estimated shape and pose using only gait parameters

(c) Estimated shape and pose using gait parameters and joint angle errors

Fig. 2: Comparison of shape and pose estimation between state models with and without joint angle errors.

configuration of the snake results in a body frame that, while dynamic with respect to the pose of any individual module, is consistent with respect to the overall shape of the snake. This virtual chassis serves to separate the internal motion of a gait itself from the external motion due to that gaits interaction in the world.

To study the effectiveness of our different body frame and state representations, motion capture data of the snake was recorded for multiple trials of the rolling gait. This data was post-processed and used as ground truth to evaluate the accuracy of the state estimates generated from the proprioceptive sensor data from the snake robot. Our results show a significant improvement in the accuracy of the estimation of pitch and roll using the virtual chassis, especially at high speeds of rolling. We also show that gait parameters can sufficiently approximate the snake robot's shape to accurately estimate pitch and roll, without having to explicitly track and estimate each individual joint angle.

II. Prior Work

There is a significant amount prior work in the study of the motion of biological snakes [5] [6] and snake robots [1] [7], these being a only selection of the works available. More recent research on both biological snakes [8] and robotic snakes [9] [10] has focused on a snake's interaction with its environment during locomotion. Our work differs significantly from these approaches in that we do not directly consider robot interaction with the world. Instead, the goal of our work is to use the virtual chassis as a means to apply simple motion models to what are traditionally considered complex systems.

A number of methods exist for fusing redundant data in robotics systems [11]. One of the most commonly used methods of fusing redundant and complimentary sensor data is the Kalman filter. The EKF extends the Kalman filter to non-linear systems by linearizing the system at the current state estimate at each time step [12].

III. State Estimation

In the following sections, it is important to note that the process and measurement models are treated identically when using both the fixed body frame and the virtual chassis. The accuracy of the underlying assumptions of these models (constant body frame angular velocities and zero body frame acceleration) are what will lead to the difference in performance between the two different body frames.

A. Gait Equation

To attain manipulation and mobility in three dimensions, our snake robots consist of 16 modules where the joints are alternately oriented in the lateral and dorsal planes of the snake [2]. Because of this design, our framework for gaits consists of separate parameterized sine waves that propagate through the lateral (even-numbered) and dorsal (odd-numbered) joints, based on Hirose's serpenoid curve [7]. We refer to this framework as the *compound serpenoid curve*,

$$\bar{\theta}(n,t) = \begin{cases} \beta_{\text{odd}} + A_{\text{odd}}\sin(\xi_{\text{odd}}) & n \text{ odd} \\ \beta_{\text{even}} + A_{\text{even}}\sin(\xi_{\text{even}} + \delta) & n \text{ even} \end{cases} \tag{1}$$

$$\begin{aligned} \xi_{\text{odd}} &= \Omega_{\text{odd}} n + \nu_{\text{odd}} t \\ \xi_{\text{even}} &= \Omega_{\text{even}} n + \nu_{\text{even}} t. \end{aligned} \tag{2}$$

In (1) β, A and δ are respectively the angular offset, amplitude, and phase shift between the lateral and dorsal joint waves. In (2) the parameter Ω describes the spatial frequency of the macroscopic shape of the robot with respect to module number, n. The temporal component ν determines the frequency of the actuator cycles with respect to time, t.

This work focuses on the rolling gait, which is a reduced parameterization of the general gait equations (1) and (2),

$$\bar{\theta}(t) = \begin{cases} A{\cdot}\sin(\xi) & \text{odd} \\ A{\cdot}\sin(\xi + \frac{\pi}{2}) & \text{even} \end{cases} \tag{3}$$

$$\xi = \nu t. \tag{4}$$

These constraints result in an arc of constant curvature that is swept through the lateral and dorsal joints. The key to this constant curvature is that the spatial frequency Ω in (2) is set to 0, and the offset between the lateral and dorsal joint angles, δ from (1), is set to $\pi/2$ radians.

B. Process Model

The state of the snake consists of parameters that describe the orientation and shape of the snake. In this work we investigate two methods of representing the shape of the snake robot. The first state representation uses the rolling gait parameters and their first derivatives to describe the shape of the snake robot, resulting in the 11 dimensional state vector,

$$\mathbf{x} = [\ A\ \ \dot{A}\ \ \xi\ \ \dot{\xi}\ \ \mathbf{q}^T\ \ \boldsymbol{\omega}^T\ ] \tag{5}$$

where A and ξ are the gait parameters from (3), $\mathbf{q} = [\ q_1\ \ q_2\ \ q_3\ \ q_4\ ]^T$ is the orientation quaternion vector in the world frame, and $\boldsymbol{\omega} = [\ \omega_x\ \ \omega_y\ \ \omega_z\ ]^T$ are the snake robot's angular velocities in the body frame.

A more complex state representation includes an angle error term for each of the joints in the snake robot,

$$\mathbf{x} = [\ A\ \ \dot{A}\ \ \xi\ \ \dot{\xi}\ \ \mathbf{e}^T\ \ \mathbf{q}^T\ \ \boldsymbol{\omega}^T\ ] \tag{6}$$

where $\mathbf{e} = [\ e_1 \ldots e_n\ ]^T$ with n being the total number of modules in the snake robot. This formulation allows gait parameters to be fit to the snake's feedback, while at the same time allowing the true shape of the snake to be captured by the state.

Tracking individual joint angles in the estimated state plays an important role when the snake robot's shape deviates significantly from a shape that can be described by estimated gait parameters. Figure 2 shows a photo of the snake robot where a module experienced an error and bent to an extremely deviated joint angle. The images to the right of the photo show the difference in the corresponding estimated shape of the snake using gait parameters to approximate the robot's shape and using gait parameters augmented with joint angle errors.

In the process model, the gait parameters at each timestep are updated by the estimate of their derivatives, and the derivatives are assumed to be constant across timesteps,

$$\hat{A}_{\text{t}} = A_{\text{t-1}} + \dot{A}_{\text{t-1}} \cdot dt \tag{7}$$

$$\hat{\xi}_{\text{t}} = \xi_{\text{t-1}} + \dot{\xi}_{\text{t-1}} \cdot dt. \tag{8}$$

If the joint angle errors are being modeled, they are updated at each timestep according to,

$$\hat{\mathbf{e}}_{\text{t}} = \lambda \cdot \mathbf{e}_{\text{t-1}} \tag{9}$$

where λ is a coefficient that drives the angle errors towards zero. This term models the effect of the proportional controllers running on each of the snake modules that are continuously closing a control loop on commanded joint angles. This term also plays a role in ensuring that gait parameters remain the primary driver of the overall shape of the snake. A value of $\lambda = 0.95$ was found to be effective during our experiments.

The quaternion orientation of the snake is updated by the angular velocities and the update timestep, according to the discrete-time update equations,

$$\hat{\mathbf{q}}_{\text{t}} = \exp(-\frac{1}{2}\boldsymbol{\Psi} \cdot dt)\ \mathbf{q}_{\text{t-1}}. \tag{10}$$

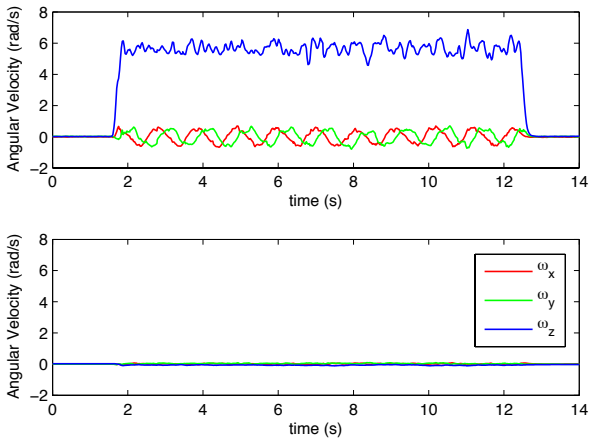

Fig. 3: A comparison of estimated angular velocities for the same motion, observed in a body frame fixed to the middle module (upper plot) and a body frame aligned with the virtual chassis (lower plot). The legend applies to both plots.

$$\boldsymbol{\Psi} = \begin{bmatrix} 0 & \omega_x & \omega_y & \omega_z \\ -\omega_x & 0 & -\omega_z & -\omega_y \\ -\omega_y & \omega_z & 0 & -\omega_x \\ -\omega_z & -\omega_y & \omega_x & 0 \end{bmatrix}. \tag{11}$$

A closed-form solution for this update is presented by van der Merwe et al. [13] that guarantees that the resulting quaternion is of unit norm.

The body frame angular velocities of the snake robot, $\boldsymbol{\omega}$, are assumed to be constant across time steps,

$$\hat{\boldsymbol{\omega}}_{\text{t}} = \boldsymbol{\omega}_{\text{t-1}}. \tag{12}$$

This constant velocity model means that only the fused sensor measurements update the estimates of body frame angular velocity. Figure 3 shows state estimates of body frame angular velocity for the same trial in both the virtual chassis and fixed body frames, and illustrates how dramatically different this assumption can be, depending on the choice of body frame.

One could argue that with the rolling gait a simple motion model could be used that predicts body frame angular velocities based on estimated gait parameters and an assumption that the snake's arc stays level with respect to the ground. Using such a process model in this case would mitigate much of the approximation error introduced by the use of a fixed body frame. However, with virtually all of the other gaits that our lab has developed [3], the motion of an individual module is more complex and any process model that updates body frame angular velocities would be dependent on gait parameters and (a mostly unknown) interaction with the world. The virtual chassis serves to inherently minimize the effects of gait motion and world interaction.

C. Observation Model

The snake robot provides feedback measurements from single-axis joint angle encoders, 3-axis accelerometers and

a 2-axis gyros located in each module. This means that the EKF measurement vector is $6n$ dimensions, where n is the total number of modules in the snake.

$$\mathbf{z} = [\ \boldsymbol{\theta}^T\ \ \boldsymbol{\alpha}^T\ \ \boldsymbol{\gamma}^T\ ]. \tag{13}$$

In (13), each element is a vector containing the measurements of a corresponding sensor type for all the modules throughout the snake robot. $\boldsymbol{\theta}$ is the vector of joint angles for each module, $\boldsymbol{\alpha}$ is the vector of accelerometer readings for each module, and $\boldsymbol{\gamma}$ is the vector of gyroscope measurements for each module.

In the measurement model, joint angles are predicted from the gait equation (3) using the current estimated gait parameters,

$$\hat{\boldsymbol{\theta}} = [\ \bar{\theta}_1 \ldots \bar{\theta}_{\mathrm{n}}\ ]^T. \tag{14}$$

If the joint angle errors are included as part of the state then the angles are predicted in same manner, but with the addition of the estimated joint angle error for each module,

$$\hat{\boldsymbol{\theta}} = [\ \bar{\theta}_1 + e_1 \ldots \bar{\theta}_{\mathrm{n}} + e_{\mathrm{n}}\ ]^T. \tag{15}$$

Predicted accelerometer and gyro readings are generated by numerically differentiating the shapes of the snake robot at different timesteps. The shape of the robot can be constructed from the forward kinematics of the joint angles predicted in (14) or (15). Using the estimated derivatives of the gait parameters, $\dot{A}$ and $\dot{\xi}$, joint angles at nearby timesteps can be generated from which the corresponding shapes can be constructed.

Predicted accelerometer measurements for each module in the snake robot are generated by combining the accelerations due to gravity (determined from the snake's estimated orientation) along with the internal accelerations due to that module's motion in the body frame

$$\hat{\boldsymbol{\alpha}}^i = \hat{\boldsymbol{\alpha}}^i_{\mathrm{gravity}} + \hat{\boldsymbol{\alpha}}^i_{\mathrm{motion}}. \tag{16}$$

Acceleration due to motion of the snake is predicted by double differentiating the estimated positions of the modules with respect to time and the world acceleration of the snake robot is assumed to be zero. The acceleration due to gravity is predicted by transforming the estimated gravity vector $\mathbf{g}$ into the frame of each module

$$\hat{\boldsymbol{\alpha}}^i_{\mathrm{gravity}} = \mathbf{M}^i\mathbf{R}\mathbf{g} \tag{17}$$

where $\mathbf{M}^i$ is the rotation matrix that describes the orientation of module i in the body frame, and $\mathbf{R}$ is the rotation matrix representation of the quaternion pose $\mathbf{q}$ in the state vector (5) or (6). For our work $\mathbf{g}$ is assumed to be oriented along the z-axis of the world frame, where g is gravitational acceleration,

$$\mathbf{g} = [\ 0\ \ 0\ \ g]^T. \tag{18}$$

The predicted gyro measurements for each module are generated by differentiating the orientation of the snake at two nearby timesteps. If $\mathbf{M}_{\mathrm{i,t}}$ and $\mathbf{M}_{\mathrm{i,t\text{-}1}}$ are rotation matrices that describe the orientations of module i in the body frame at two timesteps, then gyro measurements due to the internal

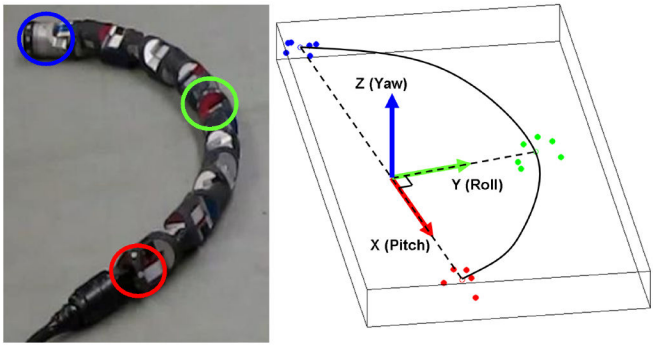

Fig. 4: Snake with IR markers and frame assignment from motion capture point clouds.

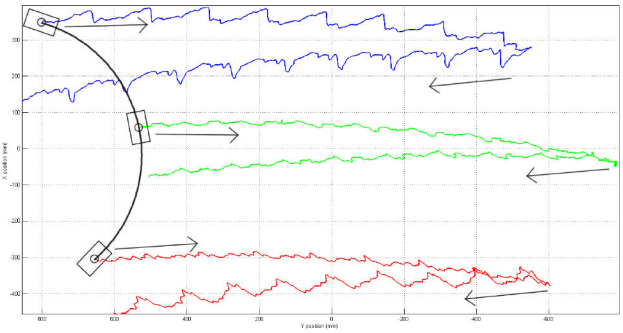

Fig. 5: A representative trajectory of a motion capture trial. The robot moves from the left to the right, then returns to the left.

motion of the gait at two timesteps, t and $t-1$ can be approximated by

$$\begin{bmatrix} 1 & -\bar{\omega}^i_{\mathrm{z}} & \bar{\omega}^i_{\mathrm{y}} \\ \bar{\omega}^i_{\mathrm{z}} & 1 & -\bar{\omega}^i_{\mathrm{x}} \\ -\bar{\omega}^i_{\mathrm{y}} & \bar{\omega}^i_{\mathrm{x}} & 1 \end{bmatrix} = \frac{\mathbf{M}^i_{\mathrm{t}}(\mathbf{M}^i_{\mathrm{t\text{-}1}})^{-1}}{dt}. \tag{19}$$

The predicted gyro measurements for each module taking into account the angular velocities of the entire robot are simply the angular velocities from (19) plus the angular velocities of the robot from the current state estimate, (5) or (6), transformed into the coordinate from of each module using $\mathbf{M}_{\mathrm{i,t}}$

$$\hat{\gamma}^i_t = \bar{\boldsymbol{\omega}}^i + (\mathbf{M}^i_{\mathrm{t}})^{-1}\hat{\boldsymbol{\omega}}_{\mathrm{t}} \tag{20}$$

The measurement model for the prediction of inertial data is where the choice of body frame comes into play. The snake's estimated body frame angular velocity affects both the predicted accelerometer and gyro measurements. The process model's assumptions of constant angular velocity between time steps is more accurate in the virtual chassis, where the frame stays relatively stable throughout its motion, compared to a fixed frame that tumbles in the world frame as a module moves.

IV. Experiment

To compare the accuracy of the various approaches for estimating the snake's pose from inertial sensors we produced ground truth data on the orientation of the snake shape

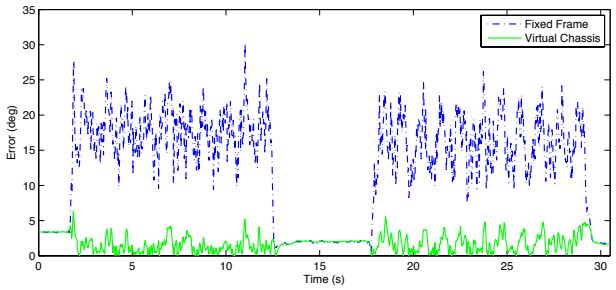

Fig. 6: Pitch error vs. time for the fixed frame and virtual chassis estimator in a fast speed trial.

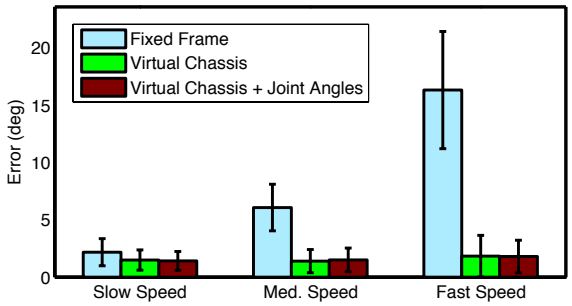

Fig. 7: Average error in estimated pitch comparing different state representations, grouped by speed of the trials.

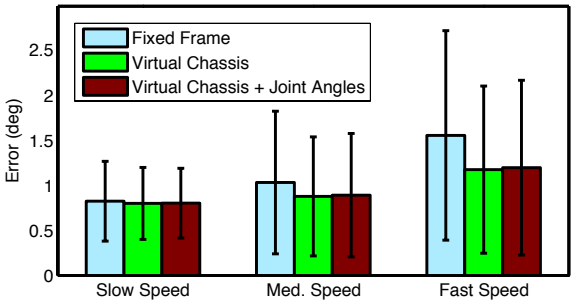

Fig. 8: Average error in estimated roll comparing different state representations, grouped by speed of the trials.

using a motion capture system. Each experiment consisted of rolling the snake across the floor with fixed commanded gait parameters. The motion capture system recorded the 3D position of IR reflective markers on three of the snake modules (head, middle, and tail) while the inertial and module angle data used for the state estimation were logged from the snake's sensors.

To compute the roll, pitch, and yaw of the snake in each frame, the motion capture point cloud data were spatially clustered into module groups. The geometric center of mass of each point cloud was used as an approximation for each module center. The measured body frame was set such that the X axis was collinear with the vector from the center of the tail to the center of the head module, and the Y axis was on the line perpendicular to the tail-head line and passing through center of the middle module (Fig. 4).

The 3D trajectories of the module centers of mass were zero-lag low passed to remove noise from IR markers rolling in and out of view of the motion capture cameras. For each of the experimental runs, the snake was driven a distance, paused, and returned to its approximate starting position (Fig. 5). Error was calculated for each of roll, pitch, and yaw by taking the absolute value of the difference between the estimated body-frame orientations and the ground truth orientations of the fitted frame.

We ran a total of 11 trials of in which we executed the rolling gait at different speeds: Slow Speed: 2 trials at 0.2 gait cycles/second, Medium Speed: 5 trials at 0.5 cycles/second, and Fast Speed: 4 trials at 1.0 cycles/second.

V. Results

Figure 6 shows a representative pitch error versus time for one of the experimental trials. In order to highlight the differences in performance of the three approaches for estimating the snake robot's orientation we only considered times when the robot was moving. For the 11 trials we computed and compared the average orientation error across different gait speeds and estimator types, as shown in Figures 7 - 9.

The state representations that used only gait parameters to approximate the shape of the snake (5) and gait parameters and joint angles offsets (6) were compared using both the virtual chassis and fixed body frames (Fig. 1) at each of these speeds. Use of the virtual chassis significantly reduced error of the estimated pitch of the snake robot. The improved accuracy of the virtual chassis was more apparent at higher speeds of rolling.

Use of virtual chassis did not improve the snake robot's average estimated yaw at at any of the different speeds that were tested. Additionally, the average and standard deviations of the errors of the yaw estimates were an order of magnitude above the errors of estimated pitch and roll. This is to be expected, as the snake's gyros and accelerometers can only provide absolute orientation with respect to gravity. Thus, the yaw orientation estimates are essentially an integration of estimated yaw velocities over the course of each trial that show significant drift due to integration error.

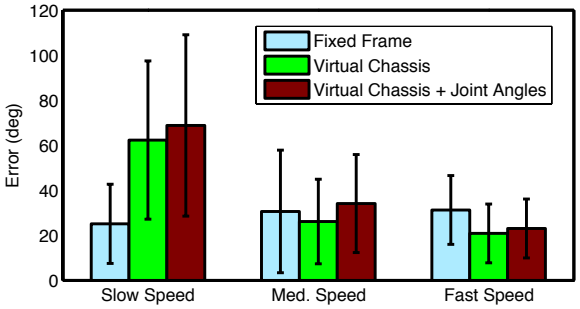

Fig. 9: Average error in estimated yaw comparing different state representations, grouped by speed of the trials.

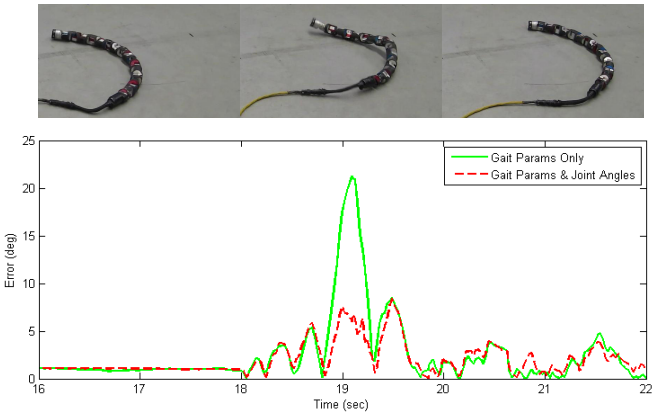

Fig. 10: Reduced error in pitch estimate by including joint angles in state.

While including joint angle deviation in the estimator state had little effect on the overall performance of the filter, it proved to have a significant effect when the snake's shape deviated drastically from the commanded gait. Figure 10 shows part of a trial where including the joint angle error improved the estimate.

VI. Conclusions

Using an EKF, we are able to successfully fuse the sensor feedback from the joint angles, accelerometers, and gyros distributed throughout a snake robot to estimate the orientation of the robot. By using the virtual chassis we are able to improve the accuracy of the snake's estimated orientation, particularly at high speeds. Additionally, we show that when the snake robot is locomoting normally, the use of gait parameters alone can sufficiently approximate the shape of the snake to accurately estimate orientation, allowing us to reduce the dimensionality of our state by more than half when considering a 16-link robot.

VII. Future Work

A. Improved Estimation Techniques

The limitations of the EKF for systems that are highly nonlinear are well documented [13]. The tendency of the EKF to diverge to incorrect state estimates was apparent while tuning the filter, especially when using a fixed body frame and for trials where the snake moved quickly. One potential improvement to this work would be to use a sigma-point Kalman filter (SPKF) to improve the accuracy of the state estimation. In particular the spherical simplex unscented Kalman filter [14] is an attractive alternative, due to the fact that it requires fewer samples of the process and measurement functions, the latter of which is computationally costly for our system.

B. Experiments with More Gaits

One eventual goal of our work is to demonstrate that using the virtual chassis in conjunction with a simplified process model can achieve accurate results over a variety of gaits. Quantitative experiments were performed using the rolling gait because it is a relatively simple locomotion that allows for an easier comparison to the ground truth data from motion capture. Future work will involve conducting more trials of the snake robots using a variety of gaits to quantify the benefits of using the virtual chassis for more complex motions.

C. Improved Ground Truth

We would also like to improve the accuracy of the ground truth data by estimating the true 6-DOF motion of each of the modules with IR markers. Work has been started on a SLAM-type approach that builds a model of how the markers are oriented on the surface of each module as the log progresses. Using those module skeletons along with the kinematic constraints of the snake mechanism should allow us to fuse the somewhat noisy and constantly occluded data of the motion capture into a more accurate estimate of the net motion and orientation of the snake.

VIII. Acknowledgements

The authors would like to acknowledge the help provided by Justin MacEy and the members of the Biorobotics Lab, particularly Ross Hatton, Matt Tesch, Mike Schwerin and Ben Brown.

References

[1] G. Chirikjian and J. Burdick, "Kinematics of hyper-redundant locomotion with applications to grasping," *International Conference on Robotics and Automation*, 1991.

[2] C. Wright, A. Johnson, A. Peck, Z. McCord, A. Naaktgeboren, P. Gianfortoni, M. Gonzalez-Rivero, R. Hatton, and H. Choset, "Design of a modular snake robot," *Proceedings of the IEEE International Conference on Intelligent Robots and Systems*, October 2007.

[3] M. Tesch, K. Lipkin, I. Brown, A. Peck, J. Rembisz, and H. Choset, "Parameterized and scripted gaits for modular snake robots," *Advanced Robotics*, 2009.

[4] D. Rollinson and H. Choset, "Virtual chassis for snake robots," in *Intelligent Robots and Systems (accepted)*, September 2011.

[5] J. Gray, "The mechanism of locomotion in snakes," *Journal of Experimental Biology*, vol. 23, pp. 101–123, December 1946.

[6] B. C. Jayne, "Kinematics of terrestrial snake locomotion," *Copiea*, no. 4, pp. 915–927, 1986.

[7] S. Hirose, *Biologically Inspired Robots*. Oxford University Press, 1993.

[8] D. Goldman and D. Hu, "Wiggling through the world," *American Scientist*, vol. 98, pp. 314–393, July 2010.

[9] A. A. Transeth, R. I. Leine, C. Glocker, and K. Y. Pettersen, "3-d snake robot motion: Nonsmooth modeling, simulation, and experiments," *IEEE Transactions on Robotics*, vol. 24, pp. 361–376, April 2008.

[10] A. A. Transeth, R. I. Leine, C. Glocker, and K. Y. Pettersen, "Snake robot obstacle-aided locomotion: Modeling, simulations and experiments," *IEEE Transactions on Robotics*, vol. 24, pp. 88–104, February 2008.

[11] R. C. Luo, C.-C. Yih, and K. L. Su, "Multisensor fusion and integration: Approaches, multisensor fusion and integration: Approaches, applications, and future research directions," *IEEE Sensors Journal*, vol. 2, April 2002.

[12] H. Choset, K. M. Lynch, S. Hutchinson, G. Kantor, W. Burgard, L. E. Kavraki, and S. Thrun, *Principles of Robot Motion*. The MIT Press, 2005.

[13] R. van der Merwe, E. A. Wan, and S. I. Julier, "Sigma-point kalman filters for nonlinear estimation and sensor-fusion - applications to integrated navigation," *Proc. AIAA Guidance Navigation and Controls Conf.*, March 2004.

[14] S. Julier, "The spherical simplex unscented transformation," in *Proceedings of the American Control Conference*, June 2003.